Control of colloids with gravity, temperature gradients, and electric fields

2003 J. Phys.: Condens. Matter 15 S11

(http://iopscience.iop.org/0953-8984/15/1/302)

INSTITUTE OF PHYSICS PUBLISHING JOURNAL OF PHYSICS: CONDENSED MATTER

J. Phys.: Condens. Matter **15** (2003) S11–S18 PII: S0953-8984(03)54828-7

Control of colloids with gravity, temperature gradients, and electric fields

Matt Sullivan[1], Kun Zhao[1], Christopher Harrison[1], Robert H Austin[1], Mischa Megens[1], Andrew Hollingsworth[2], William B Russel[2], Zhengdong Cheng[3], Thomas Mason[3] and P M Chaikin[1,3]

[1] Department of Physics, Princeton University, Princeton, NJ 08534, USA
[2] Department of Chemical Engineering, Princeton University, Princeton, NJ 08534, USA
[3] ExxonMobil Research, Annandale, NJ, USA

Received 16 October 2002
Published 16 December 2002
Online at stacks.iop.org/JPhysCM/15/S11

Abstract

We have used a variety of different applied fields to control the density, growth, and structure of colloidal crystals. Gravity exerts a body force proportional to the buoyant mass and in equilibrium produces a height-dependent concentration profile. A similar body force can be obtained with electric fields on charged particles (electrophoresis), a temperature gradient on all particles, or an electric field gradient on uncharged particles (dielectrophoresis). The last is particularly interesting since its magnitude and sign can be changed by tuning the applied frequency. We study these effects in bulk (making 'dielectrophoretic bottles' or traps), to control concentration profiles during nucleation and growth and near surfaces. We also study control of non-spherical and optically anisotropic particles with the light field from laser tweezers.

(Some figures in this article are in colour only in the electronic version)

There are several reasons to try to gain control over density, position, and motion of colloidal particles. From a fundamental standpoint, colloidal systems, especially hard spheres, serve as a paradigm for understanding the liquid, glass, and crystal phases and their transitions [1–7]. Hard-sphere systems are completely entropic and the only relevant thermodynamic variable is the volume fraction or particle density. It is therefore of some interest to find ways to control the density and density gradients which determine phases and the growth of one phase from another. Although it is almost possible to density match hard-sphere systems to prevent sedimentation, most samples settle into an equilibrium density profile. To eliminate sedimentation, experiments have been performed in microgravity. While these allow well defined densities, the growth of crystals from shear-melted samples is uncontrolled. Here we explore the use of electric fields and temperature gradients to control density and crystal growth.

On the other hand, from a practical standpoint we would like to develop a 'colloidal architecture'—a set of building blocks and tools for constructing complex objects and machines

from submicron particles. We are therefore interested not only in density control of spherical particles but also in positioning, and dynamically translating and rotating spheres and less isotropic objects. The last part of this paper addresses our study of the fabrication and manipulation of disc-shaped colloidal particles. Laser tweezers are used to trap and move particles directly. But here we show that a stationary trap can induce periodic translational motion when forcing a disc-like particle against a constraint and induce rotation in optically anisotropic discs in a circularly polarized trap.

Interparticle potentials consist of a long-range attractive interaction and a short-range repulsive interaction. When we learn elementary physics we spend most of our time discussing the different long-range attractions: e.g. van der Waals and Coulomb, and simply put in a short-range repulsion which is faster to guarantee that the system does not collapse to zero. (e.g. Lennard-Jones $a/r^{12} - b/r^6$ where the r^{-6} is justified as van der Waals and the r^{-12} is *ad hoc*). The short-range repulsion comes from a combination of the Coulomb repulsion of the electrons and the kinetic energy cost from the uncertainty principle. It rises rapidly as soon as electron orbitals start to overlap. In fact the repulsive part of the interaction is usually far more interesting than the attractive part [8]. The attractive part is responsible for the gas–liquid condensation. The repulsive part is responsible for the correlations between the particles in the condensed liquid, the liquid–crystal and glass transitions, and most of the structural correlations in matter. The simplest form of the short-range repulsive interaction is the hard-sphere interaction $V = 0$: $r_{12} > d$, $V = \infty, r_{12} < d$, where r_{12} is the interparticle separation and d is the particle diameter. Since this interaction has no finite value there is no way that it can be compared with temperature as we would do in searching for phase transitions as a function of temperature. The free energy is entirely entropic, temperature sets the only energy scale, and properties are proportional to temperature; e.g. the osmotic pressure, an energy density, is $\Pi = Z(\phi)nk_BT$. The only thermodynamic variable that determines the phase is the volume fraction, $\phi = nv_0$, where n the particle number density and v_0 the particle volume. As evidence that only repulsive interactions are required for solidification, the hard-sphere system undergoes a freezing transition to a crystalline phase, from entropy only, as ϕ passes through $\sim$0.5. The osmotic pressure for a hard-sphere system is shown in figure 1. The discontinuity from 0.496 to 0.545 is due to the liquid–crystal transition with liquid below, crystal above, and coexistence between.

The osmotic pressure can be qualitatively understood by the excluded-volume argument used by van der Waals in writing his equation of state. The pressure of a system is the volume derivative of its entropy and the entropy is proportional to the volume available for the particles. In an ideal gas the entropy is $\ln V$. It was suggested by van der Waals that once the particles have a finite size, the volume available is reduced by the volume taken up by the particles, Nv_0, to give $S = \ln(V - Nv_0) = \ln(V(1 - \phi/\phi_c))$, $\Pi = nk_BT/(1 - \phi/\phi_c)$. This result is exact in one dimension and the exact form for any dimension, d, in the limit $\phi \to \phi_c$: $\Pi = dnk_BT/(\phi_c - \phi)$, where ϕ_c is the close-packed volume fraction. Note the divergence at $\phi_c = 0.7404$ (FCC close packing) in figure 1. The random close packing of spheres relevant in the liquid state is $\phi_c = 0.636$, while 2:1 oblate ellipsoids pack to 0.68 (m&m's). Since $\phi_{ccrystal} > \phi_{cliquid}$, $S_{crystal} > S_{liquid}$ as $\phi \to 0.636$, entropy drives a liquid-to-crystal transition at $\phi < 0.636$.

Some early studies of colloidal particles as hard-sphere systems carried out to study the crystal–liquid transition were by Pusey and van Megan [2, 3]. Although their particles were not density matched and settled, they were able to demonstrate agreement with the calculated phase boundary. The existence of a density profile in their study is indicated by the existence of liquid above solid and crystal above glass in their photographs. We decided to use the equilibrium sedimentation profile in order to study the phase boundary and the interparticle

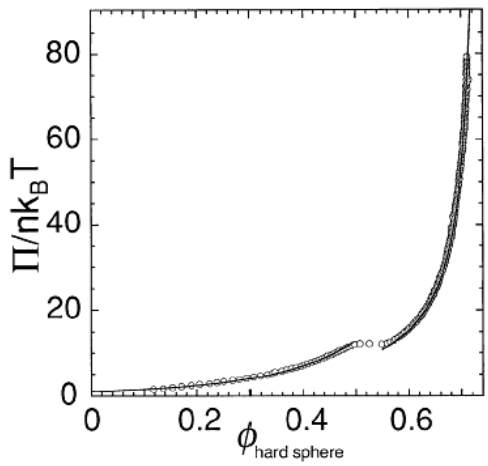

Figure 1. The equation of state (osmotic pressure as a function of volume fraction) for a hard-sphere system. The solid curve is from computer calculations. The data are from a sedimentation experiment on 15 μm diameter polystyrene spheres [10].

interactions directly. In equilibrium in a gravitational field, the weight of all particles above any horizontal cross-section is prevented from settling by the osmotic pressure of the colloidal suspension at that height [9, 10]. Therefore a measurement of the density profile versus height and knowledge of the buoyant mass of the particles can be combined to find the complete equation of state, Π versus ϕ. The circles in figure 1 are the measurements for polystyrene spheres in water (with a very small Debye screening length). The fact that they follow the solid curve (calculated) shows that the particle interactions are simply hard sphere. And the fact that the coexistence region agrees with the calculations confirms the hard-sphere phase transition.

The sedimentation experiment also demonstrates that if you want to continue to use colloids as model hard-sphere systems to study growth and dynamics at a fixed volume fraction rather than in a density gradient, you have to do something about gravity. One of the best solutions is to do the experiments in microgravity. An example of an early experiment on the Space Shuttle is shown in figure 2 [11]. The sample, PMMA in an index-matching solution of decalin and tetralin, is in the coexistence region. The crystallites are growing without settling and the experiment revealed a dendritic instability [12]. In gravity, the stress of the falling crystallite is sufficient to rip off the arms. In microgravity, we can have a system without density gradients, but we cannot control the growth. Several studies were performed by shear melting the samples to the metastable supercooled liquid state and letting them nucleate and grow [12–15]. That is the right way to learn about the fundamental physics of the problem. But in some cases, and especially to grow more perfect crystals, we would like controlled growth without instabilities. The way conventional crystals are grown is from a thermally controlled melt. As we have seen, temperature is not a control parameter for the phases of our system. However, temperature gradients are [16]!

The osmotic pressure is proportional to temperature. If we heat one end of a sample the pressure rises and the particles move down the gradient until mechanical equilibrium is achieved. This occurs when the osmotic pressure is constant, a situation which requires a higher volume fraction on the cold side than the warm side. This is shown schematically in figure 3(a) with the large single crystals that result from this growth (without dendrites) shown

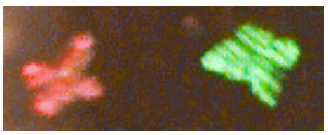

Figure 2. 1 mm crystals grown in microgravity show dendritic arms from growth instability.

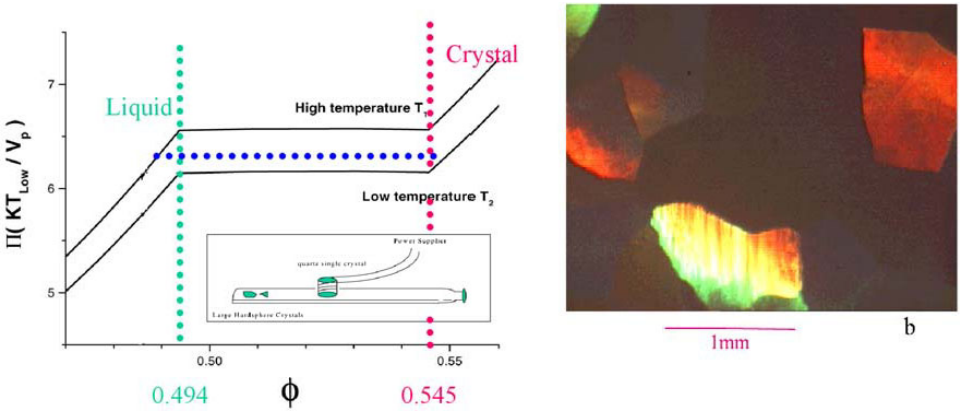

Figure 3. Left: the osmotic pressure on the two ends of the sample cell are shifted by the temperature difference. Mechanical equilibrium then sets the concentrations, one in liquid and the other in the solid phase. The inset shows the configuration for the experiment. A heater is placed toward the centre of a flat sample cell initially in the liquid state and crystals grow on the ends. Right: crystals grown on the cold side.

in figure 3(b). The process is ideally done in microgravity to avoid convection, but would take a long time since the diffusive response to the gradient is slow. Our experiment in an almost density-matched colloidal system generated slight convection from the density mismatch that actually sped up the process considerably.

While temperature gradients are useful, they are limited by the freezing and boiling points of the solvent. To get stronger effects we decided to try electric fields and dielectrophoresis. By now the dielectrophoretic trapping is probably best understood in colloidal science by analogy to laser tweezers. Tweezers work by bringing a laser beam to focus with a microscope objective. There is an intense high-frequency electric field at the focus and a large gradient. Particles with positive dielectric constant ε have energy $(-\varepsilon E^2/2)$ in the field and are attracted to the highest field, at the focal point, with a force $\sim\varepsilon\nabla(E^2/2)v_0$. Similarly if we use a set of parallel plates we can make a 'dielectrophoretic bottle'. Between the plates the field is constant, so the particles experience no force and the physics is simply determined by their volume fraction. However, their density is higher between the plates than outside by a Boltzmann factor equal to $\exp(-\varepsilon v_0 E^2/2k_BT)$ in the dilute limit. For more concentrated samples we must equate osmotic pressure or chemical potential. At the edges of the plates a field gradient produces a force that tends to pump the particles into the bottle.

The experimental configuration is shown schematically in figure 4 along with confocal images of the particles. The density difference between in and out of the trap/bottle is evident and at first glance the abruptness of the transition region is striking. When the field is turned off the particles quickly relax to their uniform horizontal distribution with no crystals in the sample. The expected density profile can be obtained from the pressure balance:

$$\frac{\partial \Pi}{\partial x} = \frac{n}{2}\frac{\partial(\delta\varepsilon\, E^2)v_0}{\partial x} = \frac{\varphi}{2}\frac{\partial\, \delta\varepsilon\, E^2}{\partial x}$$

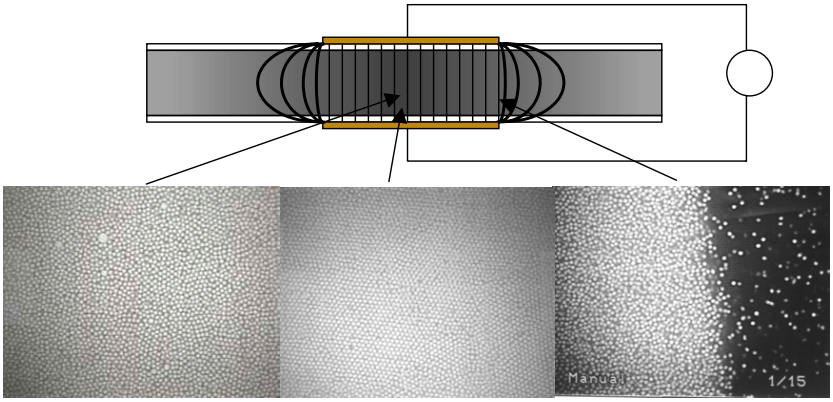

Figure 4. The 'dielectrophoretic bottle'. The schematic diagram shows the capacitor plates (outside the cover slips) and the electric field lines. The confocal images on the left and right illustrate the density profile about ten particle layers up from the bottom cover slip. The middle image was taken at ∼5 layers in, where the density is slightly higher due to gravity.

or equating the chemical potential throughout the system:

$$\mu_0 = \mu(\phi) + v_0 \frac{\delta\varepsilon\, E(x)^2}{2}.$$

Here $\delta\varepsilon$ is the difference in dielectric constant between the colloidal particle and the solvent. Interestingly $\delta\varepsilon$ is frequency dependent, mostly due to the conductivity, σ (however slight), of the solvent. We should treat $\delta\varepsilon$ self-consistently. Taking the real part the Clausius–Mossotti equation yields

$$\mathrm{Re}\left(\frac{\varepsilon_p^* - \varepsilon_m^*}{\varepsilon_p^* + 2\varepsilon_m^*}\right) = \frac{(\sigma_p - \sigma_m)}{(1+\omega^2\tau^2)(\sigma_p + 2\sigma_m)} + \frac{\omega^2\tau^2(\varepsilon_p - \varepsilon_m)}{(1+\omega^2\tau^2)(\sigma_p + 2\sigma_m)}$$

where the subscripts p and m correspond to particle and solvent respectively. For most samples, $\delta\varepsilon = \varepsilon_m\,\mathrm{Re}((\varepsilon_p - \varepsilon_m)/(\varepsilon_p + 2\varepsilon_m))$ can be adjusted through zero in the frequency range 1–10^7 Hz.

Confocal images of different parts of the sample are also shown in figure 4. The density can be varied readily from less than 1% to above the crystallization concentration ∼0.54. When the microscope is focused through the sample we see no signs of stringing or clumping of the particles in the dilute phase, in the gradient region, or in the dense liquid and crystal regions within the electric bottle. Again the method is most applicable in a microgravity or density-matched sample. For the sample of 1 μm PMMA in decalin, the particles sediment as the gravitational height is ∼10 μm. For the density-matched sample the dynamics would again be controlled by diffusion and would be very slow. The gravitationally driven height profile however allows for a much faster equilibration process. The dielectrophoretic force acting on each particle creates a body force on the fluid that is stronger toward the bottom of the sample. The dense sediment is convected toward the high-field region. We could use the equations above with an additional term for the gravity field and solve the complete profile, but for illustrative purposes we test them at fixed height, where the equations should work as written. In figure 5 we show the horizontal density profile for two different heights. The dielectric mismatch at this frequency is ∼0.2 and the voltage applied across the gap (∼500 μm) between the gold electrodes (placed on the outside of the glass cover slips to prevent contact with the colloid) is 200 V and at 250 kHz. The only adjustable parameter is the slight horizontal

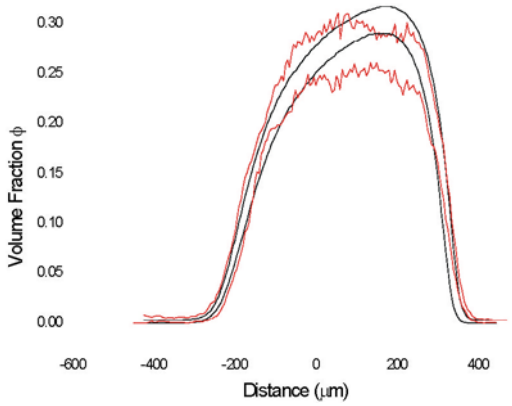

Figure 5. The horizontal density profile at ∼3 monolayers (upper) and 5 layers (lower) from the bottom of the sample cell. Curves with noise are data, solid curves are calculated with one fit parameter, the offset of the capacitor plates.

offset of the two electrodes which causes the pattern to be skewed. The fit works better than we could have expected.

The geometry that we use for this experiment is similar to what is found in experiments on electrorheological fluids where the particles form strings due to the induced dipolar interaction. Why do we not get strings (which would prevent the use of this technique to study non-interacting hard spheres)? To get a sizable change in the volume fraction we need an interaction with the applied field which is greater than $k_B T$. To avoid stringing we need a dipole–dipole interaction much less than $k_B T$. The total dipole moment of a dielectric sphere (in vacuum) in a uniform field is

$$P_{tot} = \frac{(\varepsilon - 1)}{(\varepsilon + 2)} E r^3.$$

The energy in the field is

$$P_{tot} E = \frac{(\varepsilon - 1)}{(\varepsilon + 2)} E^2 r^3 \sim \frac{\delta\varepsilon}{3} E^2 r^3.$$

The dipole–dipole interaction of two touching dipoles with their centres along the field direction is

$$\frac{2P_{tot}^2}{(2r)^3} = \frac{\left(\frac{(\varepsilon-1)}{(\varepsilon+2)}\right)^2 E^2 r^6}{4r^3} \sim \frac{(\delta\varepsilon)^2}{36} E^2 r^3.$$

Therefore we can use dielectrophoresis to control the particle density without stringing if we have $\delta\varepsilon \ll 12$, more generally $\delta\varepsilon/\varepsilon_m \ll 12$.

We have also been interested in using laser tweezers to control the positions and motions of our particles and in using non-spherical particles for our studies. In figure 6 we show some 2 μm diameter by 0.4 μm thickness discs/doughnuts which we have fabricated by photolithography. For experiments, we can fabricate about 10^8 discs at a time. We have used several different materials including PMMA. When trapped in laser tweezers such discs sit 'edge on' with respect to the flat surface of the objective (like a coin standing up on a table) or parallel to the average direction of light propagation [17]. They undergo Brownian rotational diffusion about the axis of the tweezing light. Light scatters forward from the face of the discs in two streaks which are easy to track and yields a sensitive measure of the particle orientation. Backscattered light from the disc edges is easily observable as streaks using the

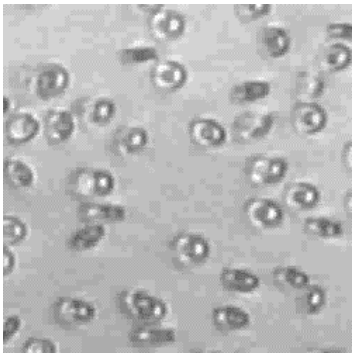

Figure 6. 2 μm $\times$ 0.4 μm SiN colloidal discs/doughnuts fabricated by photolithography. Similar discs have been made with PMMA.

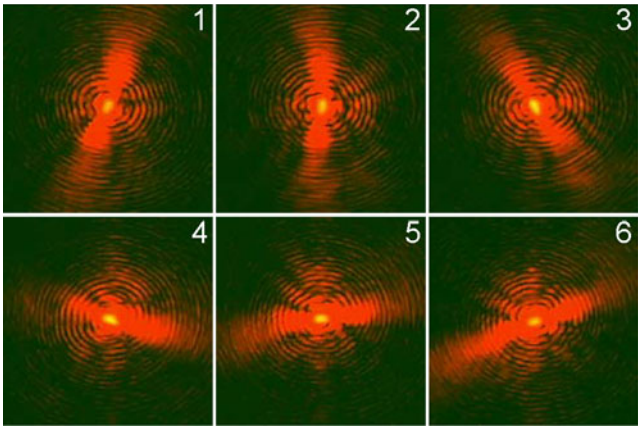

Figure 7. The colloidal lighthouse. Eicosene discs backscatter light from the disc edge and undergo forced rotation in circularly polarized light while held edge on in an optical tweezer.

microscope. Discs made from birefringent particles are also trapped edge on, but align with the polarization of the linearly polarized light. They undergo hindered rotation in angular analogy to a harmonically bound Brownian diffuser. When circularly polarized light is applied there is a torque on the particles and they spin on their axis at a rotation rate which is proportional to the applied power. Figure 7 shows stills from the rotation.

Finally, when the particles are forced to touch the back cover slip, they undergo a translational 'switchback motion [17]. The tweezers acting on the disc push it against the constraint and it tilts from its edge-on configuration. Once there is an angle between the disc and the average direction of propagation of the light, there is a lateral force from photons bouncing (reflecting) off the disc face (i.e. a transverse photon pressure). The disc starts translating out of the beam, undergoes a torque from friction on the cover slip, and both a restoring force and a restoring torque from the tweezers. At a critical value of the 'friction', the coupled equations are unstable and a combined rotational–translational periodic motion starts. The frequency is linear in the applied power or photon pressure. Thus it is possible to get interesting and complex motion even from a stationary light field on colloidal particles.

In conclusion, we have demonstrated that colloidal particles can be manipulated in bulk or individually with a variety of applied fields and that micron size particles can be fabricated with a variety of shapes and optical properties. These techniques should allow the construction

of interesting static and dynamic structures—colloidal architecture, and should be useful for a number of fundamental studies.

Acknowledgments

We acknowledge support from NASA and ExxonMobil.

References

[1] Hansen J-P and McDonald L R 1986 *Theory of Simple Liquids* (New York: Academic)
[2] Pusey P N and van Megan W 1986 *Nature* **320** 340
[3] Pusey P N 1991 *Liquids, Freezing, and Glass Transition* ed J-P Hansen, D Levesque and J Zinn-Justin (Amsterdam: Elsevier) ch 10 pp 763–941
Anderson V J and Lekkerkerker H N W 2002 *Nature* **416** 811
[4] Debenedetti P G 1996 *Metastable Liquids: Concepts and Principles* (Princeton, NJ: Princeton University Press)
[5] Russel W B 1990 *Phase Transit.* **21** 27
[6] Weeks E R, Crocker J C, Levitt A C, Schofield A and Weitz D A 2000 *Science* **287** 627
[7] Kegel W K and van Blaaderen A 2000 *Science* **287** 290
[8] Chaikin P M 2000 *Soft and Fragile Matter, Nonequilibrium Dynamics, Metastability and Flow* ed M E Cates and M R Evans (Bristol: Institute of Physics Publishing)
[9] Piazza R, Bellini T and Degiorgio V 1993 *Phys. Rev. Lett.* **71** 4267
[10] Rutgers M A, Dunsmuir J H, Xue J-Z, Russel W B and Chaikin P M 1996 *Phys. Rev.* E **53** 5043
[11] Zhu J, Li M, Rogers R, Meyer W V, Ottewill R H, Russel W B and Chaikin P M 1997 *Nature* **387** 883
[12] Russel W B, Chaikin P M, Zhu J, Meyer W V and Rogers R 1997 *Langmuir* **13** 3871
[13] Ackerson B J and Schätzel K 1995 *Phys. Rev.* E **52** 6448
Ackerson B J and Schätzel K 1992 *Phys. Rev. Lett.* **68** 337
Ackerson B J and Schätzel K 1993 *Phys. Rev.* E **48** 3766
[14] Palberg T 1999 *J. Phys.: Condens. Matter* **11** R323
[15] Cheng Zhengdong, Chaikin P M, Zhu Jixiang, Russel W B and Meyer W V 2002 *Phys. Rev. Lett.* **88** 015501
[16] Cheng Z, Russel W B and Chaikin P M 1999 *Nature* **401** 893–5
[17] Cheng Z, Chaikin P M and Mason T G 2002 *Phys. Rev. Lett.* **89** 108303